Pediatric Radiology (2022) 52:2038–2050
https://doi.org/10.1007/s00247-022-05412-9

THORACIC IMAGING

Pediatric lung ultrasonography: current perspectives

Deeksha Bhalla[1] · Priyanka Naranje[1] · Manisha Jana[1] · Ashu Seith Bhalla[1]

Received: 2 November 2021 / Revised: 5 May 2022 / Accepted: 31 May 2022 / Published online: 18 June 2022

Abstract
Ultrasonography (US) is the workhorse of pediatric imaging; however, lung US is only a recently developed application. US of the lung is based predominantly on the imaging of chest wall–air–fluid interfaces. In this review, we summarize the available literature on applications of lung US in neonatal as well as pediatric care. We describe the imaging appearance of various commonly encountered pathologies including pneumonia and respiratory distress syndrome, among others, and provide illustrative images. Finally, we describe the limitations of the technique that are essential knowledge for radiologists, critical care physicians, sonographers and technologists attempting to use lung US effectively for diagnosis and management.

Keywords Chest wall · Children · Infants · Lung · Neonates · Respiratory distress syndrome · Technique · Ultrasound

Introduction

Since the introduction of "artifact imaging" by Lichtenstein et al. [1] for recognition of lung pathology on US, lung US has gained momentum as a leading modality in the critical care setting. Lung US has proved to be of considerable value in adult intensive care units (ICUs), and extensive research has gone into extending the same concepts to the care of sick newborns and older children who require urgent diagnosis and frequent monitoring [2–4].

In children, along with being an inexpensive, portable and sensitive technique, US has the advantage of being free of ionizing radiation, making lung US particularly appealing. However, several limitations such as lack of appropriate transducers and inadequate operator training or experience have limited its use to tertiary-care and specialized centers. In this review, we summarize the available literature on use of lung US in neonatal as well as pediatric patients. We also seek to familiarize readers with the semiotics and nomenclature of lung US examinations as described in international guidelines [5, 6].

✉ Manisha Jana
manishajana@gmail.com

[1] Department of Radiodiagnosis and Interventional Radiology, All India Institute of Medical Sciences, Ansari Nagar, New Delhi 110029, India

Basics of technique and positioning

In neonates and infants, a small-footprint linear hockey stick transducer is used where available, or simply a high-frequency (10 Hz or more) linear transducer is employed [2, 6].

With increasing age, the size of the thoracic cavity increases and non-visualization of the deeper lung fields becomes a concern, and convex or micro-convex (5-MHz) probes are recommended [5]. A lung image map must be created by investigating corresponding areas in each hemithorax. The hemithorax is roughly divided using a parasternal line, and anterior and posterior axillary lines into the anterior, lateral and posterior segments (Fig. 1).

Often in critically ill children, who are limited to the supine position, only the anterior and lateral lung segments can be evaluated [7]. As much of the posterior lung as can be examined is done by turning these children onto their contralateral side and directing the probe anteriorly. Stable children can be turned to a lateral or prone position to examine the posterior lung [8, 9]. Five basic imaging findings must be recognized [6]:

a) Lung sliding: The to-and-fro motion of visceral pleural line against chest wall with respiration. On M mode imaging, this appears as the "seashore sign" (Fig. 2, Online Supplementary Material 1).
b) A lines: Horizontal, hyperechogenic lines parallel to the pleural line. A lines with lung sliding form the normal lung signature (Fig. 2).
c) B lines: Hyperechogenic lines that are perpendicular to the pleura and move with lung sliding (Fig. 3). Might

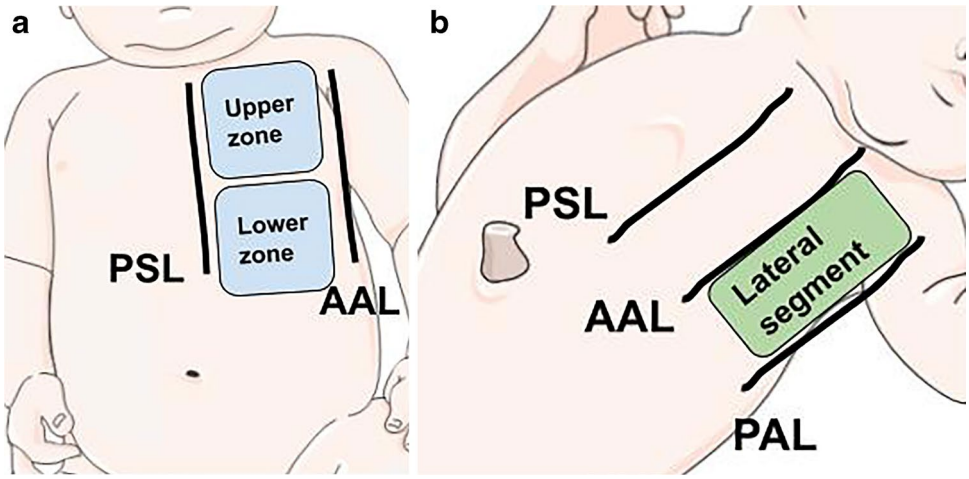

Fig. 1 Scanning technique in lung US. Diagram shows the lung is divided into anterior, lateral and posterior segments by three lines, the parasternal line (*PSL*), anterior axillary line (*AAL*) and posterior axillary line (*PAL*). **a** The anterior lung lies between the parasternal line and anterior axillary line and is roughly divided along the nipple line into upper and lower zones. **b** The lateral lung lies between the anterior axillary line and posterior axillary line. Posterior lung lies posterior to the PAL. In a critical care setting, examination is usually restricted to supine position and only anterior and lateral segments are examined. In other situations, the child might be turned over and posterior lung might be examined with similar division as anterior lung

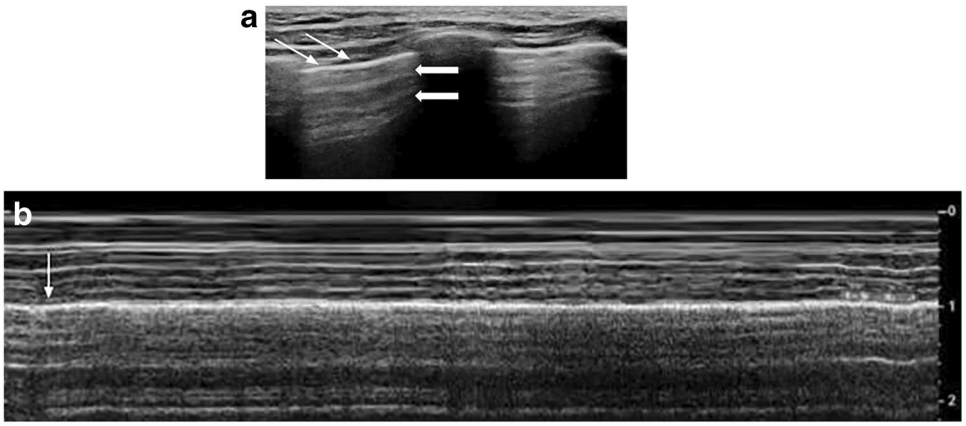

Fig. 2 Normal pleural line and lung sliding in a 3-year-old girl. **a** Longitudinal US image shows pleural line as a regular, thin, echogenic interface (*thin arrows*) that moves to and fro with respiration. A lines are the reverberation artifact of the pleura produced by aerated lung (*thick arrows*). These are horizontal parallel lines that decrease in frequency with increasing depth from the pleural surface. **b** On M mode, the granular echogenicity of the lung (*arrow*) abutting the pleura is depicted by the "seashore sign." In comparison, the static chest wall produces the "waves"

be present and normal in the first 48 h after birth. They represent interstitial fluid accumulation or rarely scarring.

d) Consolidation: Density of lung resembling solid tissue, referred to as "hepatization." Tiny, branching, hyperechoic "air bronchograms" might be evident within the consolidated lung (Fig. 3).
e) Pleural effusion: Presents as separation of the visceral and pleural lines by anechoic fluid, known as the "quad sign" in dependent locations. On M mode, the "sinusoid sign" is formed by periodic motion of the visceral pleura toward the parietal pleura with each respiratory cycle (Fig. 4).

Applications

Neonates

Lung US has transformed the management of respiratory distress syndrome (RDS) in both term and preterm neonates. The use of lung US for predicting complications of RDS such as bronchopulmonary dysplasia is well accepted. Authors have

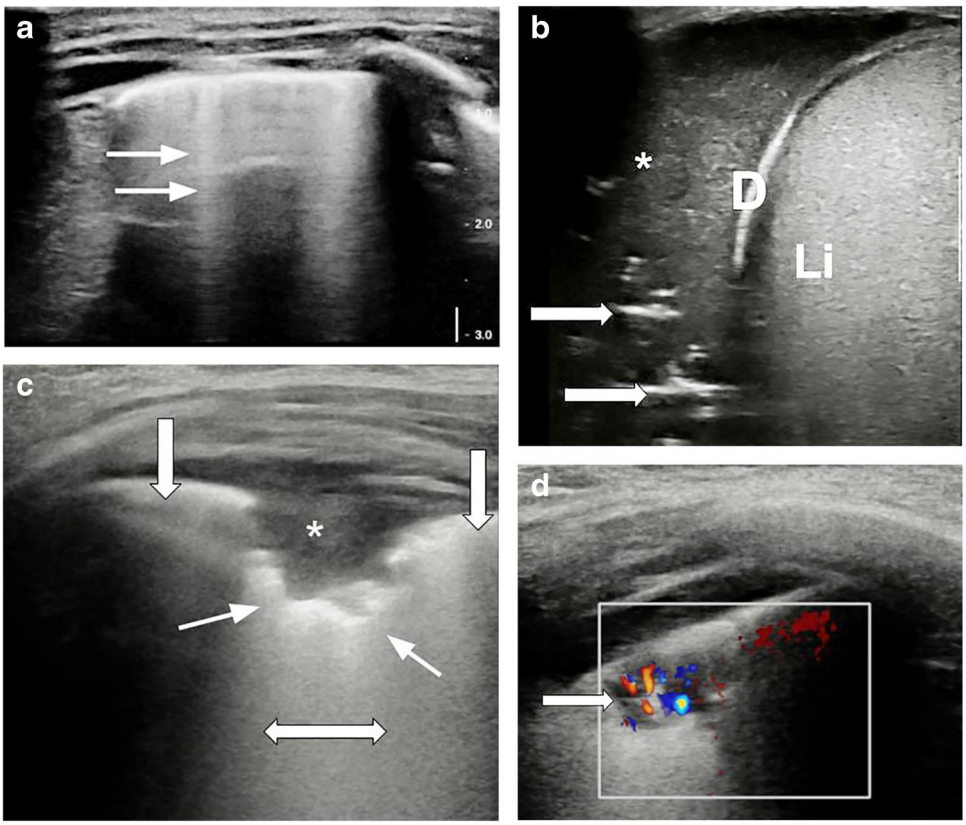

Fig. 3 B lines and consolidation in a 5-year-old girl. **a** Axial US image of the anterior upper lung shows normal B lines (*arrows*). These are the comet tail artifacts that arise at the pleural surface and are oriented perpendicular to it. They erase A lines and move with lung sliding. **b** Longitudinal US image of the posterior lower lung depicts a patch of consolidation, or an appearance of lung echogenicity that resembles solid tissue (*), also known as "hepatization of lung." Multiple branching hyperechoic structures, or air bronchograms (*arrows*), are evident within it. These are dynamic and move with respiration. *D* diaphragm, *Li* liver. **c** Axial US image shows a small subpleural consolidation (*), causing a break in continuity of the pleural line (*thick arrows*). At the base of consolidation, the pleural line appears torn or shredded (*thin arrows*), referred to as the "shred sign." Deeper to it, note the confluent B lines (*double-arrow*). **d** Color Doppler US interrogation in the axial plane using intercostal approach. Image shows a peripheral consolidation with normal branching vascularity (*arrow*), which is a useful tool to differentiate consolidation from an infarct

reported 100% positive predictive value of lung US for complications of RDS [10]. Persistence of retro-diaphragmatic hyperechogenicity beyond day 9 is the earliest predictor for development of bronchopulmonary dysplasia [11]. This refers to appearance of a sharp hyperechoic line with reverberation artifact (B lines) behind the diaphragm in transhepatic or transsplenic scanning, that is, in the visualized lung base (Fig. 5).

In addition, there has been an emerging concept of therapy decision-making and monitoring based on lung US. While initial studies described a pattern approach to predict the need for ICU admission and mechanical ventilation [12], a paper by Brat et al. [3] provided a quantitative assessment of lung aeration that correlated with oxygenation indices and need for surfactant in neonates with RDS. They additionally considered consolidation as an indicator for poor aeration along with the "severe B pattern," i.e. coalescent B lines. They reported 100% sensitivity in predicting surfactant requirement in neonates with gestational age (GA) <34 weeks. De Martino et al. [2] also reported a high accuracy of 89% in predicting surfactant need in very preterm (<30 weeks GA) neonates.

The appearance of other common neonatal respiratory disorders such as transient tachypnea of newborn (TTN) and meconium aspiration syndrome (MAS) has also been described [13, 14]. The former presents as pulmonary interstitial syndrome, with "white lung" showing coalescent B lines in severe cases and characteristic absence of consolidation. The "double lung point" has a high specificity (94.8%) for diagnosis of TTN. It refers to an appearance of the lung at a point where there is intersection of the inferior lung, with very compact B lines and the superior lung, which shows more widely spaced B lines (Figs. 6 and 7). In a head-to-head comparison among patients with TTN and RDS, consolidations with air bronchograms were seen only in RDS, while double lung point was seen only in TTN and not in RDS [15]. MAS, on the other hand, consistently shows consolidation with air bronchograms. Atelectasis might be evident in severe cases.

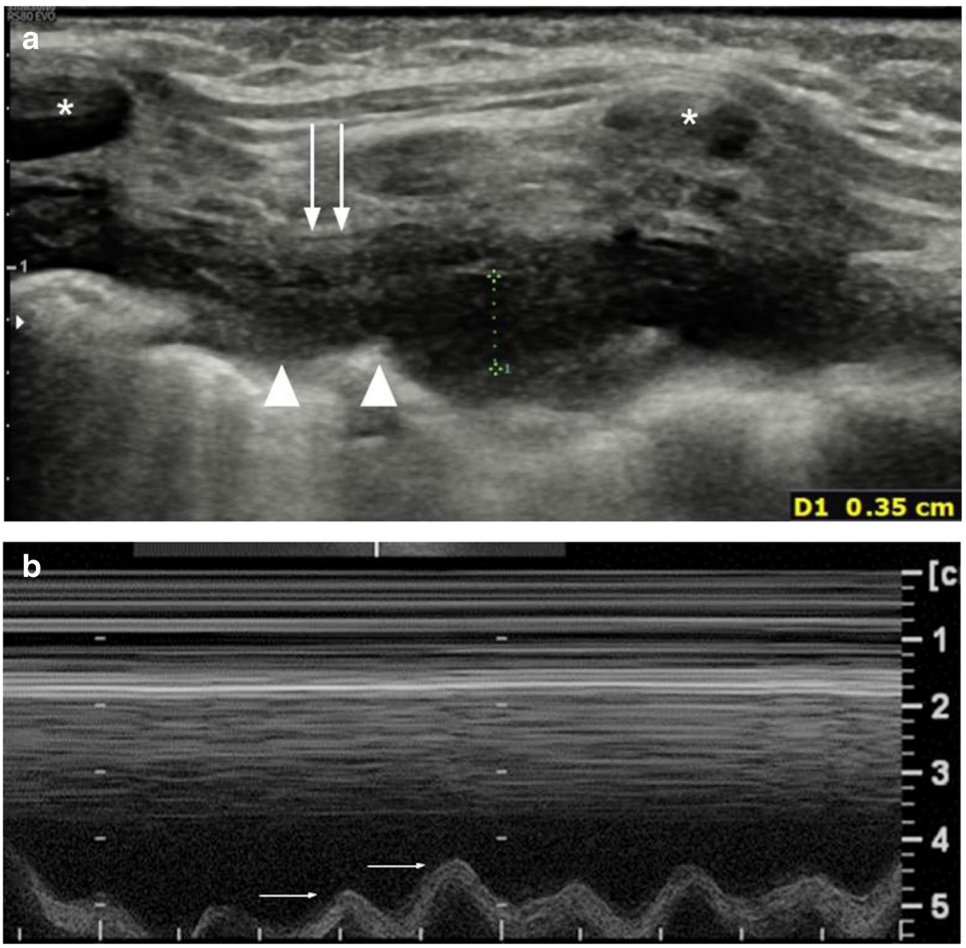

Fig. 4 Pleural effusion on lung US in a 4-year-old girl. **a** The "quad sign" is formed in the longitudinal plane by fluid separating the visceral and parietal pleura (*cursor*). The four sides are formed by the two ribs (*), the visceral pleural line (*arrows*) and the parietal pleural line (*arrowheads*). **b** On M mode imaging, the "sinusoid sign" is evident — the undulating appearance of the pleural line (*arrows*) caused by respiratory phasic variation in distance between visceral and parietal pleura

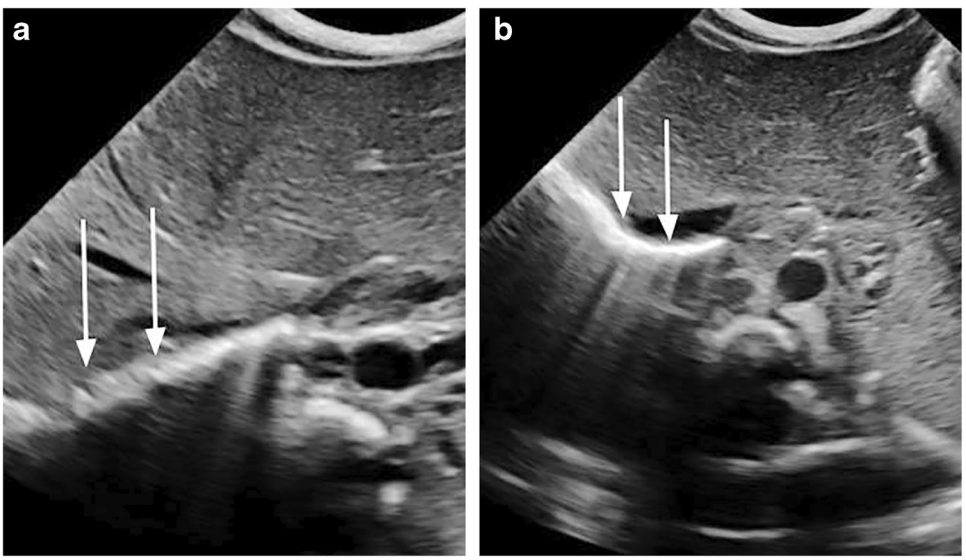

Fig. 5 Retrodiaphragmatic hyperechogenicity on lung US in a 3-week-old boy. **a** Longitudinal transhepatic image shows the normal diaphragmatic line (*arrows*) with aerated lung behind it. **b** The appearance of increased B lines in the lung behind the diaphragmatic line (*arrows*) on longitudinal transhepatic scan is referred to as "retrodiaphragmatic echogenicity"

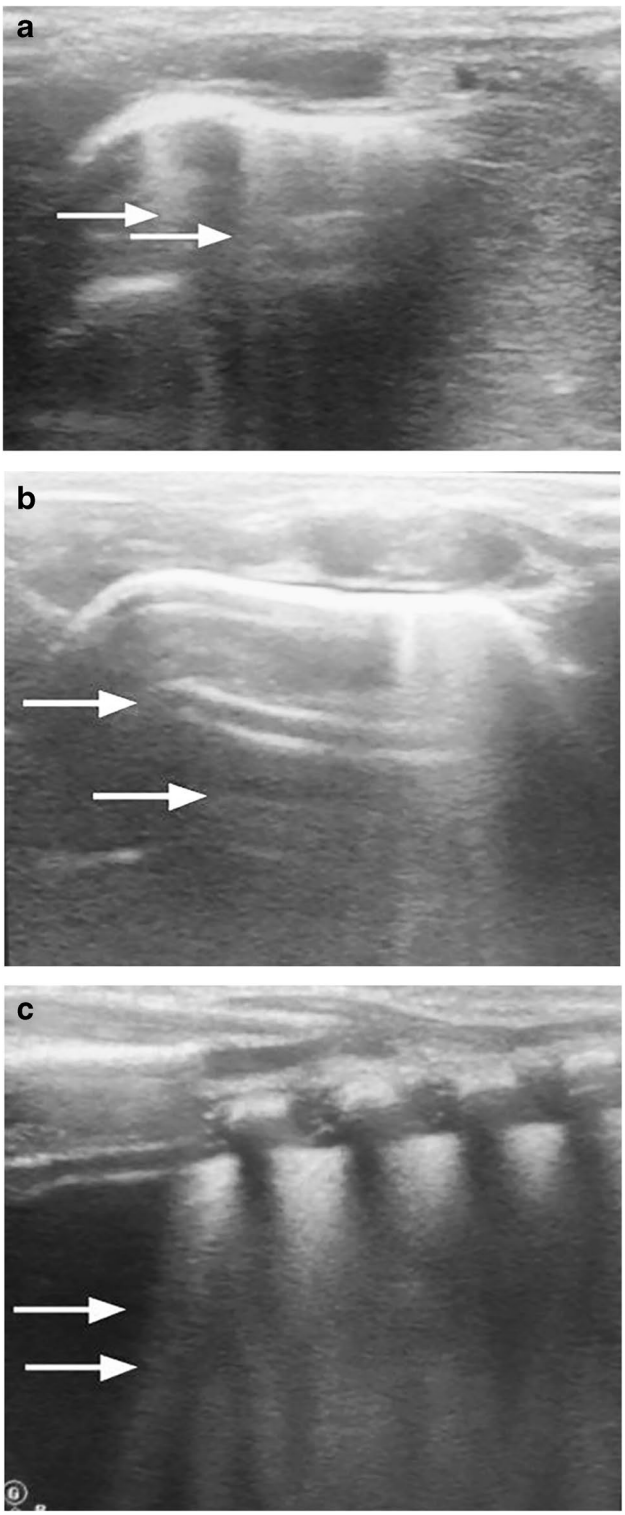

Fig. 6 Transient tachypnea of newborn in a girl born at 37 weeks of gestation who had respiratory distress 48 h after birth. **a** Axial US of inferior lung through the anterior intercostal window shows multiple compact B lines (*arrows*) with a paucity of A lines. **b** Axial US of the superior lung shows predominantly A lines (*arrows*) with a few widely spaced B lines. **c** Longitudinal plane US depicts "double lung point" (*arrows*), where the superior lung with normal A lines meets the inferior lung with compact B lines that erase the normal A lines. There was a resolution of respiratory distress in 48 h

There has been encouraging evidence on adapting lung US for neonatal RDS surveillance. Brusa et al. [16] observed substantial interobserver agreement between beginner-level and expert interpreters, which increased to excellent level when an intermediate-level operator was tested.

Critical care

The applications of lung US to critical care in children are similar to those in adults. They include conditions such as pneumothorax, pulmonary edema and hemorrhage. The reach of US in the pediatric intensive care unit (PICU) and neonatal intensive care unit (NICU) is now expanding beyond radiologists to critical care providers, pediatric cardiologists and emergency physicians. Given that the purpose of these exams is not to perform a comprehensive lung evaluation but instead to answer specific clinical questions, time is of the essence. The bedside lung US in emergency (BLUE) protocol can help to systematically gather the maximum information in the shortest possible time [17]. The scan time is typically less than 3 min [18].

In this protocol, the appearance is divided into seven profiles, beginning with the examination of lung sliding, A lines, B lines and effusion along the anterior aspects and progressing posterolaterally, with the last step being confirmation of venous patency in the lower limbs. In the absence of anterior lung sliding, a lung point, i.e. the intersection of absent lung sliding with normal lung sliding, was 100% specific for showing pneumothorax with a reported sensitivity of 88% (Online Supplementary Material 2). In fact, lung US showed excellent performance even in radiographically occult pneumothoraces, with 79% sensitivity for these as well. Absent lung sliding without a lung point was seen in patients with asthma; however, these patients could also have a normal lung profile. In cases of intact lung sliding, anterior B lines were sought, the presence of which denoted cardiogenic pulmonary edema with a sensitivity of 97% and specificity of 95%. Normal lung sliding, with normal A lines, i.e. a normal anterior lung profile, in a patient with venous thrombosis was highly specific (99%) for pulmonary embolism [18]. Pneumonia could have a wide variety of appearances including anterior consolidations, asymmetrical lung profiles and the posterolateral alveolar and/or pleural syndrome, referred to as PLAPS. Posterolateral alveolar pleural syndrome is labeled when the lung shows tissue-like density (alveolar consolidation), along with the shred sign, which is an irregular line between the normal aerated lung and the tissue pattern of consolidated lung (Fig. 3) [19]. This is most common in the posterior dependent lung, referred to as the "PLAPS point." This might be accompanied by pleural effusion. Other concerns in the ICU such as endobronchial intubation, foreign

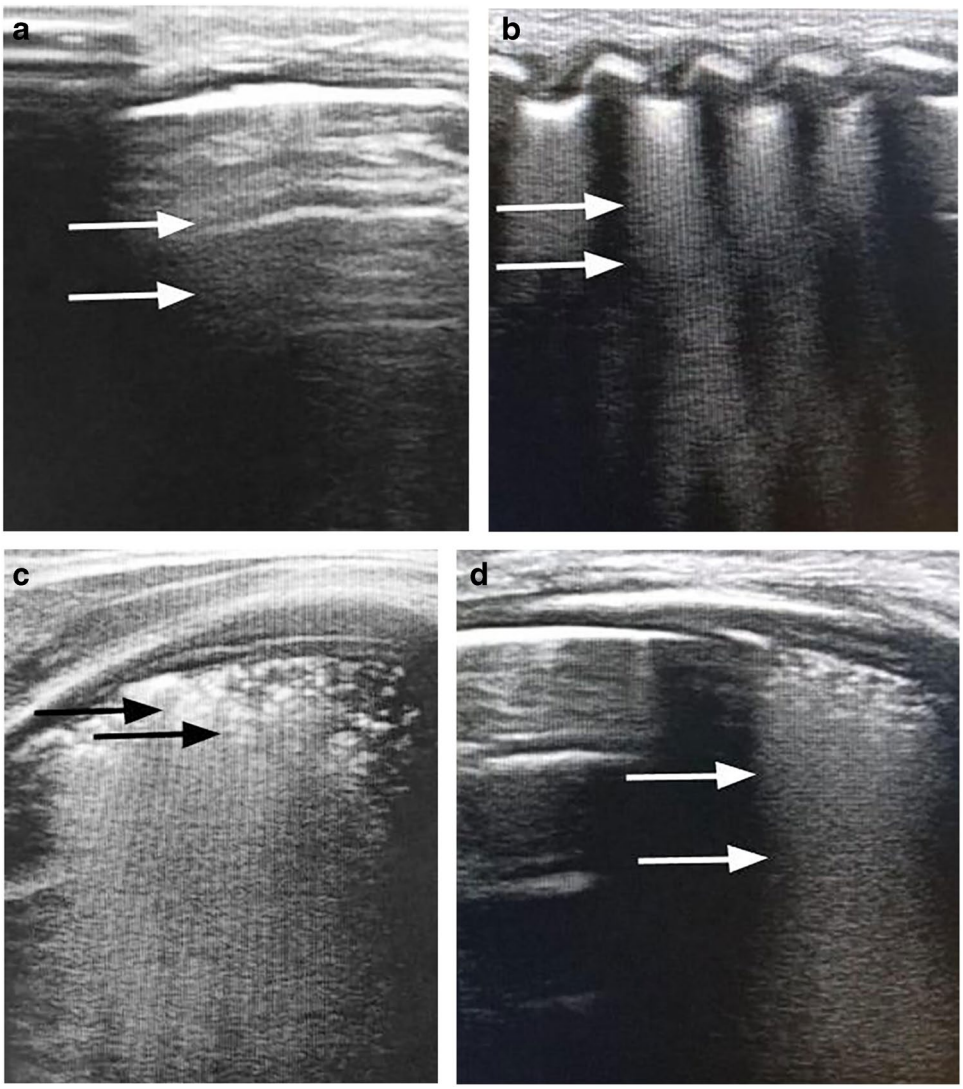

Fig. 7 Transient tachypnea of newborn in a term male neonate at 48 h with respiratory distress. **a** Axial US of anterior lung along the superior aspect shows normal A lines (*arrows*). **b** Similar to the girl in Fig. 6, longitudinal plane US shows that there are coalescent B lines in the inferior lung field (*arrows*). **c** Axial US of the inferior lung field also shows subpleural consolidations with air bronchograms (*arrows*). **d** A "double lung point" is noted on longitudinal US, where the normal A lines and the coalescent B lines intersect (*arrows*). Based on the double lung point, the boy was diagnosed with transient tachypnea of newborn. There was resolution of the respiratory distress in 48 h with supportive therapy

body aspiration or mucus plugs in airways can also be immediately addressed. There is immediate appearance of the "lung pulse" in atelectasis. This refers to synchronous beating of the lung with cardiac activity, which is caused by the transmitted heart pulsation via a collapsed lung along with abolished lung sliding. The lung pulse itself has 90% sensitivity for atelectasis [20].

Pneumonia

The summary of evidence on the use of lung US for diagnosing childhood pneumonia yielded high pooled sensitivity (96%) and specificity (93%) versus a reference standard of chest radiographs, clinical criteria or both. Among neonates alone, the estimates of pooled sensitivity and specificity rose to 96% and 100%, respectively. However, the caveat to these estimates, particularly in neonates, is the overlapping appearance of many disorders such as MAS, RDS and hemorrhage, which also present with consolidation on lung US as described here. Thus, consideration of clinical criteria is essential before any lung consolidation can be labeled as pneumonia.

An important consideration is differentiation of consolidation from atelectasis, which is based on the dynamic air bronchograms evident in consolidations. These show respiratory variation, while static air bronchograms are evident in atelectasis. Atelectasis also shows the presence of a lung pulse, as described earlier.

An inherent limitation of lung US is that it can only diagnose consolidations that reach the pleural surface and lie in the intercostal window. In adults, the estimate of such missed consolidations is 8% [21]. In children, this concern is less; however, lung US performs poorly in certain areas such as the lung apices, left lower lobe and lung hila [22].

Another concern is the diagnosis of interstitial pneumonia on lung US (Figs. 8 and 9). This is usually caused by viral pathogens and presents as an alveolar interstitial pattern on lung US with an increased number of coalescent B lines [23]. Significant interobserver variability occurs in the interpretation

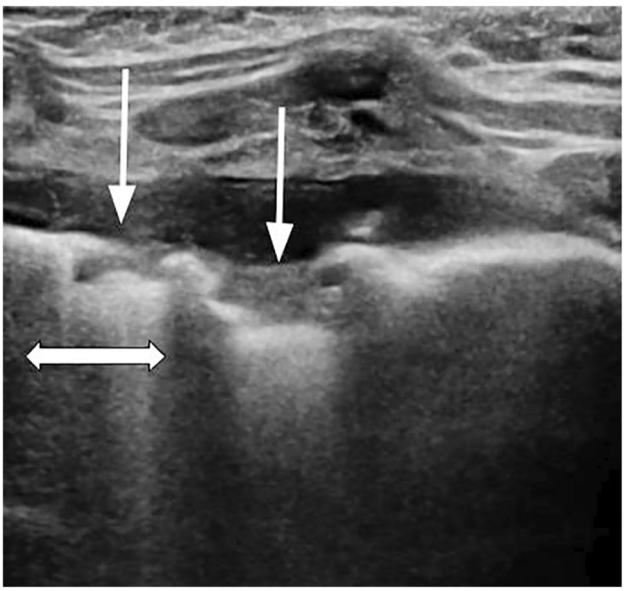

Fig. 8 Viral bronchiolitis in a 4-year-old girl. Axial US shows small subpleural consolidation (*arrows*), seen as a break in continuity in the solid pleural line (shred sign). There are areas of confluent B lines underneath (*double-arrow*), suggesting an interstitial process

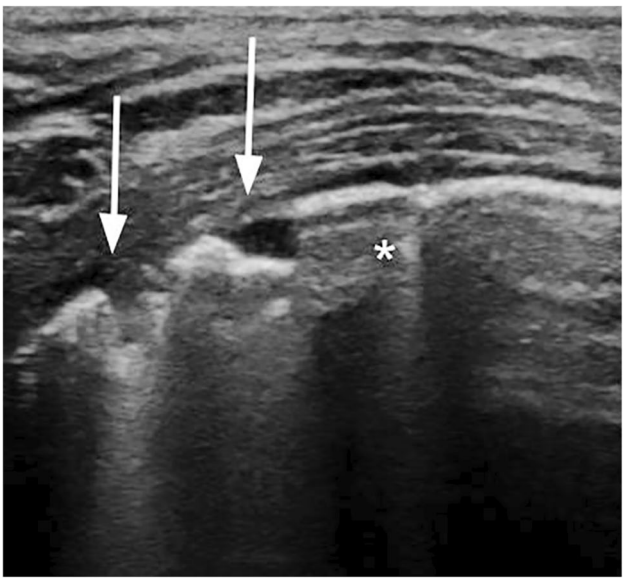

Fig. 9 Viral bronchiolitis in an 11-year-old girl. Axial scan shows small subpleural consolidation (*arrows*) with B lines in underlying lung. Note the normal aerated lung adjacent to the consolidation (*)

of the number of B lines and distance between them [24, 25]. This difference might be rarely clinically important, however, because most children spontaneously recover from these infections in the absence of any comorbidities.

It is also of note that the reference standard against which lung US is compared is CT in most studies, the accepted gold standard for depiction of lung involvement. However, it is neither possible to transport all sick children to CT scanners nor ethical to expose them to ionizing radiation just for the purpose of validating research. In a prospective study by Ambroggio et al. [26], CT was performed for clinical reasons in 27% patients, while the probability of CT findings was statistically calculated in the others. Lung US and radiographs both showed statistically similar sensitivity for detecting consolidation, interstitial disease and pleural effusion compared to CT scan, while radiographs had slightly higher sensitivity for findings such as masses (Fig. 10) [26]. The specificity of radiographs was significantly higher for excluding interstitial pneumonia and pleural effusion. The inter-rater reliability (IRR) of lung US and radiographs was also estimated. Lung US showed moderate IRR (0.55) for consolidation and poor IRR for interstitial pneumonia (0.32) [26]. The IRR for chest radiographs showed the reverse: it was substantial for interstitial disease (0.63) and poor for consolidation (0.35) [26].

Lung US also has a role in complications of pneumonia (Fig. 11) and their management. US aids the differentiation of lung abscess from empyema based on appearance at color Doppler US. While an abscess shows color flow from the residual necrotic lung parenchyma, empyemas are avascular [27]. The use of lung US for therapeutic decisions in parapneumonic effusions has also been studied. A statistically significant difference was noted between US grading of pleural echogenicity (greater or lesser than 50%) and the presence of pleural organisms, longer treatment durations and need for redo procedures [28]. A detailed discussion of treatment of parapneumonic effusions and empyema is beyond the scope of this article.

Wheezing in children

In the initial description of utility of lung US in children with bronchiolitis by Caiulo and colleagues [29], they described a correlation between the clinical disease severity and the lung US findings. In children with mild bronchiolitis, there was predominance of scattered B lines. As the severity increased, more children showed subpleural consolidation and areas of white lung. Pleural line abnormalities were also seen [29]. However, there was differing opinion among several authors, who argued that these findings could be incidental and the correlation was not easily established [30, 31].

In recent work by La Regina et al. [32], the authors also performed lung US in controls, who showed none of the abnormalities seen in patients with bronchiolitis, thus validating the findings of Caiulo et al. [29]. They also assigned a lung US score, similar to the score used by Brat et al. [3], where higher score was assigned to confluent B lines and widespread B lines and larger consolidations [32]. This score showed correlation with clinical disease severity, length of hospital stay and oxygen requirement [32].

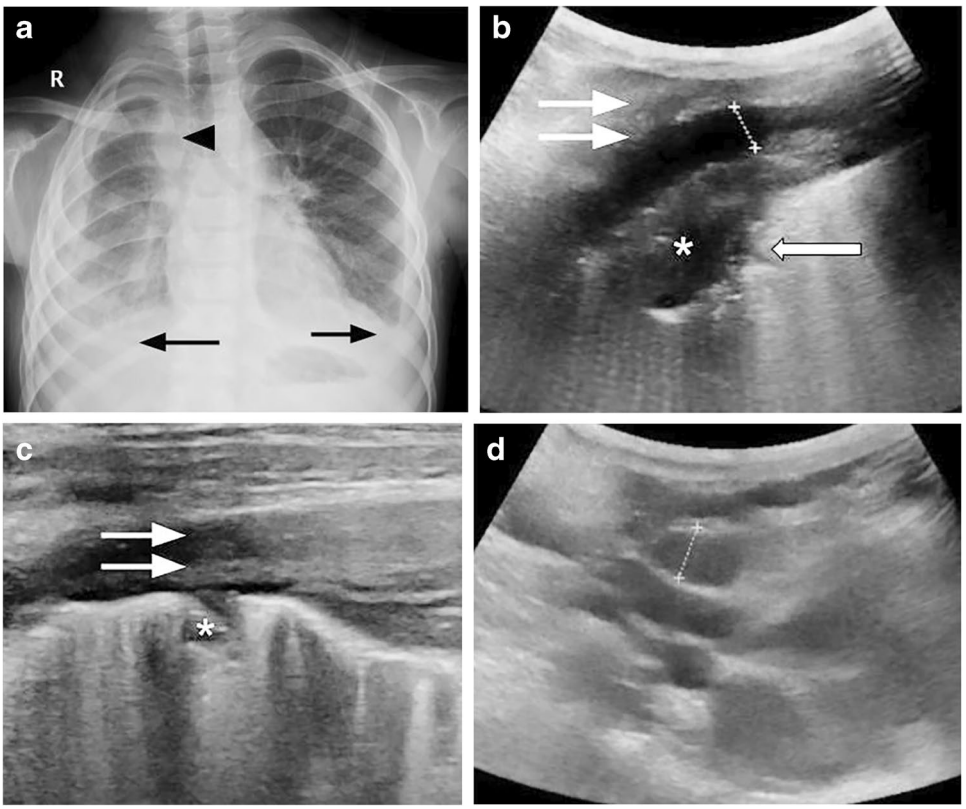

Fig. 10 *Mycobacterium tuberculosis* infection in a 12-year-old boy. **a** Anteroposterior radiograph of the boy shows bilateral cardiophrenic angle obliteration (*arrows*), with right pleural fluid extending along the lateral chest wall. Thickened right paratracheal stripe is evident (*arrowhead*) along with a hazy right lung. **b** Longitudinal US shows extensive pleural thickening (*dual arrows*) on the right side with a small effusion (*cursor*). Consolidated lung (*) is seen underneath, giving a shred sign along the interface with aerated lung (*single arrow*). **c** Axial US shows thickened pleura (*arrows*), with small consolidation (*) and interstitial syndrome in the underlying lung. **d** Longitudinal US of the mediastinum shows enlarged mediastinal lymph nodes (*cursor*) anteroinferior to the aortic arch

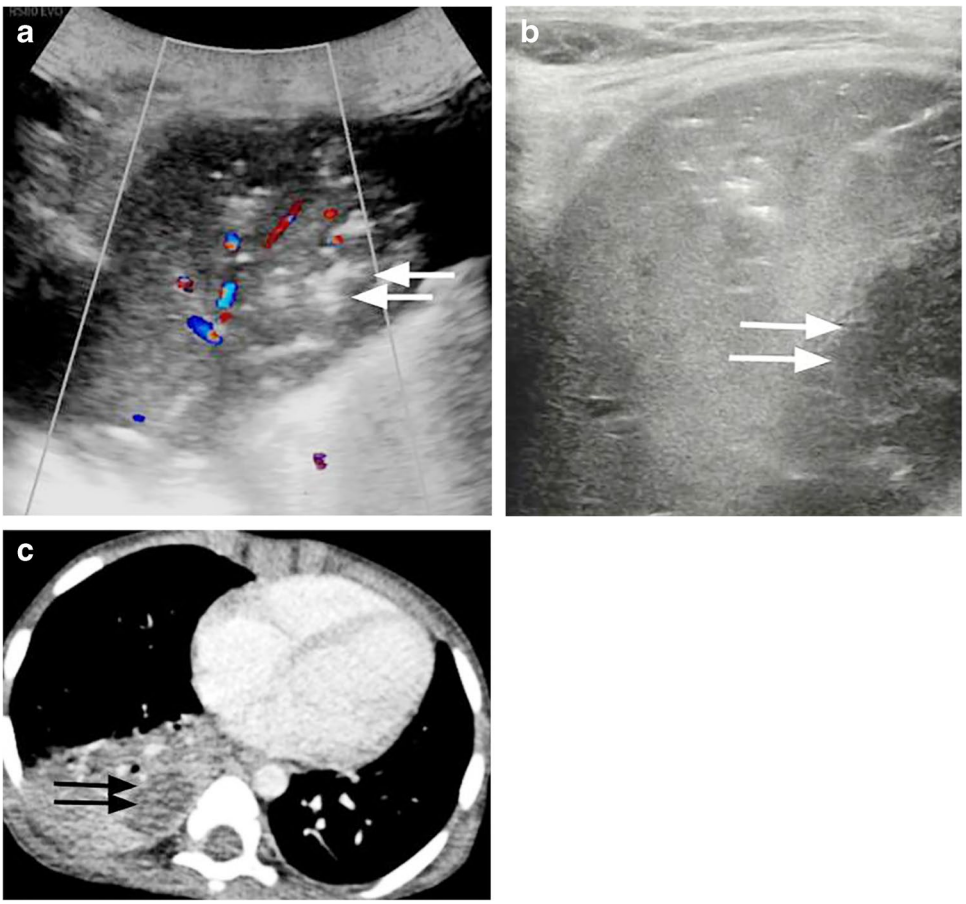

Fig. 11 Necrotizing pneumonia in a 4-year-old boy being treated for non-Hodgkin lymphoma. **a** Axial lung Doppler US shows consolidation in the right lower lung with air bronchograms (*arrows*) and characteristic branching pattern of vascularity. **b** On sagittal US section, the entire lower lobe is hepatized, with a central anechoic area (*arrows*) with an irregular margin, suggesting internal necrosis. **c** Axial enhanced CT shows the hypodense, non-enhancing area (*arrows*) within the consolidation, which confirms the US diagnosis of necrotizing pneumonia

Lung masses

In peripheral masses, lung US is an excellent modality for characterizing internal architecture (solid versus cystic) and vascularity and serves as a guide for sampling. Good tissue yield is obtained on thoracic US-guided biopsies [33], reducing need for re-biopsy.

In children, the majority of lung masses are either congenital tumors or metastatic lesions. However, primary lung masses, both aggressive and malignant, including inflammatory myofibroblastic tumor, pleuropulmonary blastoma and carcinoid tumors, form a significant minority, and lung US can be used to aid in evaluating and differentiating these from other inflammatory and benign neoplastic pathologies [34]. In a study comparing contrast-enhanced CT with thoracic US in 53 adults with bronchogenic carcinoma, US scored higher than CT in detection of peritumoral atelectasis, diaphragmatic palsy and supraclavicular lymphadenopathy, and the difference was statistically significant [33]. The same advantages might be exploited in children as well, particularly for differentiating atelectasis from tumor tissue, because this forms an essential component of tumor staging as well as accurate sampling (Fig. 12). Similar concerns exist in children with non-resolving pneumonia, which is also often caused by underlying masses. US has also shown high rates of detection of air or fluid bronchograms, a useful differentiating feature between masses and consolidation [35].

In addition, in masses that are benign or developmental, diagnosis might be forthcoming on US itself, without the need for additional investigations that require iodinated contrast agent, ionizing radiation or sedation. The foremost among these are lesions such as hydatid cysts, where US is the ideal modality for both initial classification of disease and follow-up of evolution [36].

Congenital malformations

Congenital pulmonary lesions include congenital pulmonary airway malformation (CPAM), pulmonary sequestration and congenital diaphragmatic hernia (CDH). These are usually detected and prognosticated antenatally, using a combination of US and fetal MRI.

Lung US is useful in children with recurrent pneumonia in a single lobe, where intralobar pulmonary sequestration might be the cause [37]. Extralobar pulmonary sequestration, on the other hand, can be large enough to cause neonatal respiratory distress. Anecdotal reports of large associated hydrothoraces in children with extralobar sequestration also exist and these can contribute to

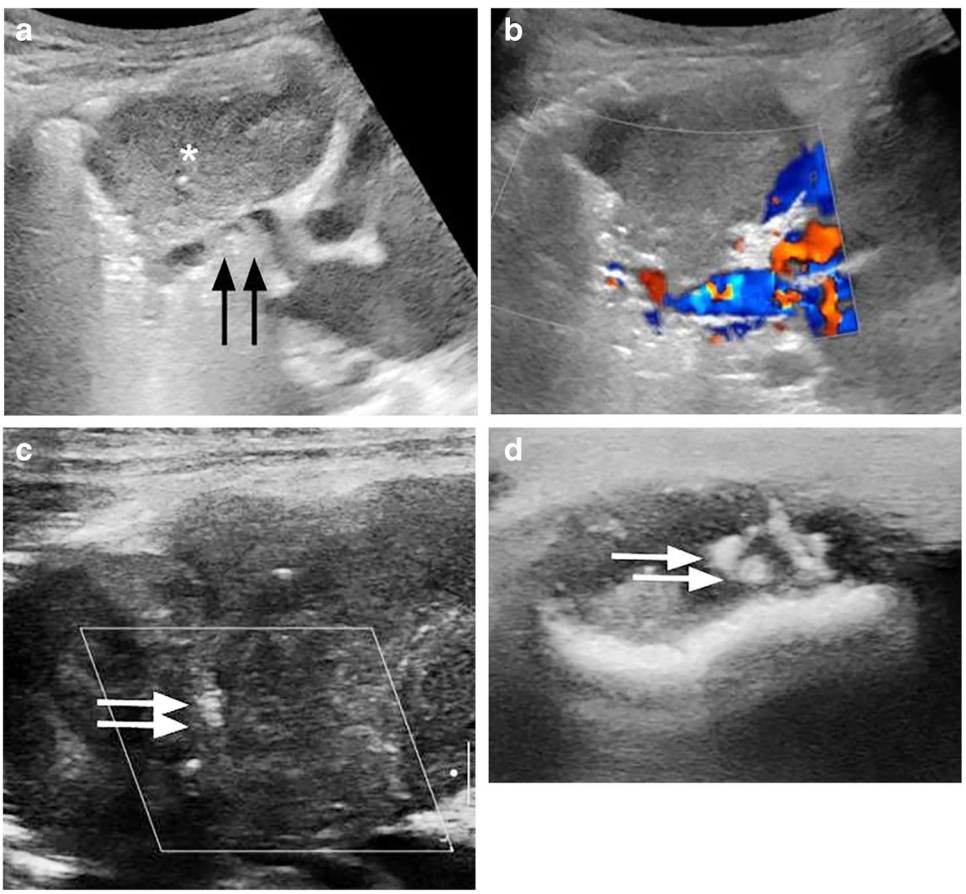

Fig. 12 Lung US for mass differentiation in a 4-year-old boy who presented with discharging sinus along the chest wall and absent breath sounds along the right anterior lung fields. **a** Longitudinal section US reveals a mass in the right lung (*), which is in close relation to the left superior pulmonary vein (*arrows*), although the fat plane is maintained. **b** Longitudinal color Doppler US image shows the preserved flow in the vein. **c** With use of the high-frequency transducer in axial plane to study internal architecture, echogenic foci are evident within the mass, suggesting calcification (*arrows*). **d** In another lesion in the scalp, axial US shows similar internal architecture, suggesting metastasis. However, biopsy taken from the lung mass under US guidance revealed necrotic epithelioid cell granulomas, suggesting disseminated tubercular infection

depressed respiratory function [38]. Doppler sonography plays a crucial role in these children, who present with solid lesions in the lung bases, by demonstrating the systemic supply from the thoracic or abdominal aorta (Fig. 13).

Congenital pulmonary airway malformation also causes respiratory distress in 50–65% of affected neonates [37]. The appearance is based on Stocker types [39]: types I and II present as complex multicystic masses with septae and mixed solid components [40]; type III lesions, on the other hand, are homogeneous solid echogenic masses but without the identifiable systemic supply. A lesion with separate solid and cystic components might represent a mixed CPAM and sequestration.

Advances in knowledge

Contrast-enhanced ultrasonography (CEUS) has emerged as a problem-solving tool in myriad conditions. It is particularly useful in children because it obviates the needs for iodinated contrast agent in children with renal impairment as well as ionizing radiation, which is especially important in children needing multiple scans. In a series of children between age 1–12 years with complicated pneumonia, CEUS helped to accurately delineate foci of necrotizing pneumonia as non-enhancing areas among sections of consolidation. In addition, it helped to demarcate areas of complex parapneumonic effusion from the lung parenchyma [41]. Intracavitary instillation of US contrast agent via the drainage catheter has also been used in children with complex effusions to identify fibrinous septae, which necessitate catheter-directed fibrinolysis. Free dispersion of microbubbles within the effusion indicates communicating loculi, which is a sign of successful therapy. Similarly, this helps to confirm catheter location and patency [42].

In the era of coronavirus disease 2019 (COVID-19), there has been extensive use of lung US in COVID care centers and ICUs as a surrogate for high-resolution CT (HRCT) scans, not just for case identification but also for treatment allocation. The "light beam" artifact is the most specific sign of pneumonia in COVID-19 infection, and this corresponds to the early appearance of ground-glass densities on the HRCT [43]. The light beam artifact is a bright, vertical echogenic band that moves with respiration. It comes and goes from the screen with lung sliding, creating an "on–off" effect. This originates from a regular pleural line with interspersed A lines and B lines. The COVID lung signature consists of patches of the light beam artifact with areas of separated and coalescent B lines, alternating with large "spared" areas. Volpicelli and colleagues [43] suggested use of the lung aeration score developed by Bouhemad and colleagues [44] to assess dynamic changes in aeration while on different ventilation strategies such as awake proning, continuous positive

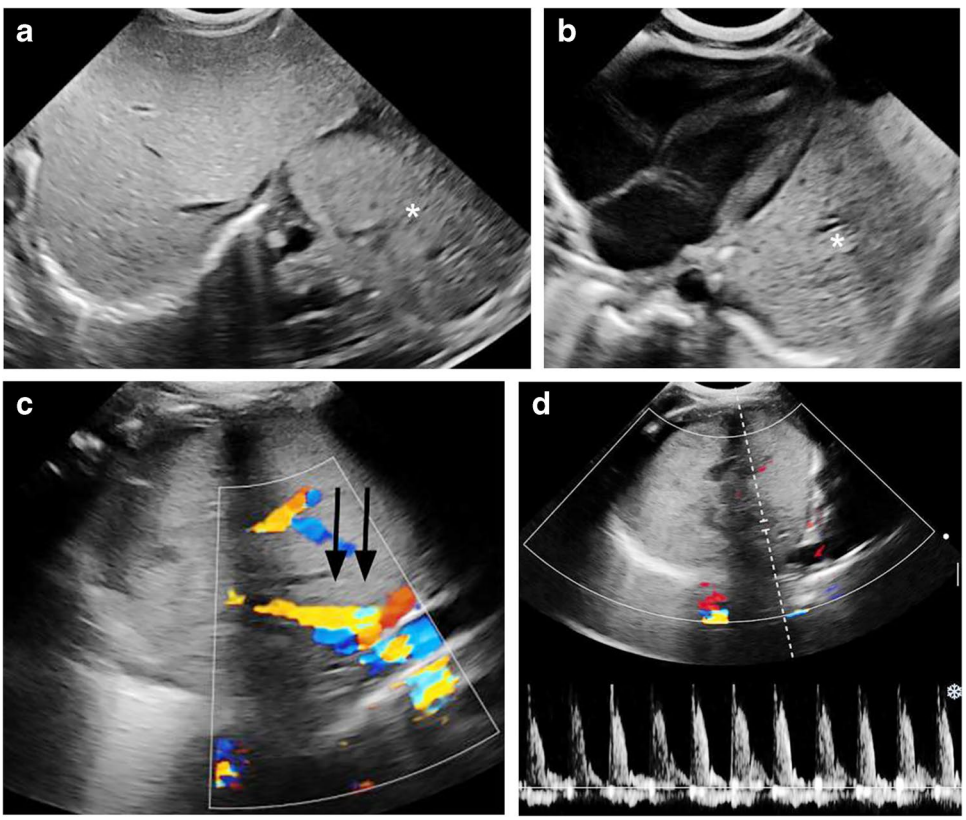

Fig. 13 Pulmonary sequestration in a 3-week-old boy. **a** Axial US through the substernal approach shows an echogenic mass (*) in the left lung base. **b** Axial US using anterior intercostal approach reveals the paracardiac location of the mass (*). **c** Longitudinal color Doppler image shows a vessel arising from the thoracic aorta to supply the mass (*arrows*), leading to the diagnosis of pulmonary sequestration. **d** Spectral Doppler in the longitudinal plane shows the low-resistance arterial waveform in the supplying vessel, as would be expected of vasculature supplying pulmonary parenchyma

airway pressure (CPAP) and invasive ventilation. This score, similar to the RDS score developed by Brat and colleagues [3], gives higher scores to areas with coalescent B lines or consolidation, lower scores to those with separated B lines, and nil to those with normal lung.

Limitations

While lung US has opened an exciting vista of possibilities for diagnosing, treating, monitoring and prognosticating a wide variety of etiologies and disease presentations, it is essential for operators to be aware of the inherent limitations of the technique as well as their own limitations while interpreting scans. Operator training and expertise are the foremost concerns, although data have emerged to suggest that US-naive operators might also be able to acquire and interpret lung US independently after performing as few as 10 supervised scans [45].

The time required to perform each scan is also an important consideration. While chest radiography takes only a couple minutes, a complete lung US can take 20 min or even more [46]. Considering this, tailored protocols to reduce the time of examination such as the BLUE protocol, described earlier, and the fluid administration limited by lung sonography (FALLS) protocol, which is a focused assessment for causes of acute circulatory failure, have been developed for critical care. However, even in elective examinations, the relative person-hour cost and throughput is an important consideration.

As mentioned, the performance of lung US for central lesions and round atelectasis is inadequate. The scapula in older children also prevents visualization of a significant part of the lung field [47]. In addition, lung US is not useful for evaluating positions of tubes and lines, such as endotracheal tubes and intercostal drainage tubes, which is an important part of ICU protocols. Many pathologies show similar appearance with variable combinations of A lines and B lines, which can be difficult to differentiate. Although high accuracy has been reported by most authors using lung US for a variety of clinical scenarios, it is well known that widespread publication bias exists for lung US and point-of-care US as a whole. Interpretation errors can occur, such as pneumothorax in the presence of subcutaneous emphysema or lung infarcts versus pneumonia.

It is thus prudent to remember that judicious use of this modality, with awareness of the pitfalls and use of radiographic and CT correlation when required, yields the highest diagnostic accuracy and clinical benefit.

Table 1 summarizes the current applications of lung US in neonates and older children. Table 2 lists common pathological conditions and their imaging appearance.

Table 1 Current applications of lung US

	Well-accepted use	Potential role
Neonates		
RDS	Prediction of complications (BPD)	Quantitative assessment of aeration and prediction of surfactant requirement
TTN	Diagnosis	
MAS	Diagnosis	
Congenital lesions	Diagnosis of CPAM and EPS	
Older children		
Pneumonia	Detection of pleural involvement (parapneumonic effusion, empyema) Diagnosis of subpleural consolidations Detection of mass in non-resolving pneumonia Detection of pulmonary sequestration in recurrent pneumonia	CEUS for identification of loculi in effusions, necrotizing pneumonia Diagnosis of interstitial pneumonia such as COVID-19
Lung masses	Differentiation of solid from cystic Guide for sampling	Detection of diaphragmatic invasion CEUS for vascularity
Critical care		
Pneumothorax	Diagnosis	Quantification and therapy monitoring
Cardiogenic pulmonary edema	Diagnosis	
Atelectasis	Differentiation from pneumonia Surrogate for airway obstruction	
ARDS	Confirmation of diagnosis	Quantification of lung aeration

ARDS acute respiratory distress syndrome, *BPD* bronchopulmonary dysplasia, *CEUS* contrast-enhanced ultrasonography, *COVID-19* coronavirus disease 2019, *CPAM* congenital pulmonary airway malformation, *EPS* extralobar pulmonary sequestration, *MAS* meconium aspiration syndrome, *RDS* respiratory distress syndrome, *TTN* transient tachypnea of newborn

Table 2 Abnormalities and key imaging findings of lung US

	Imaging appearance	Specific features
Pneumothorax	Absent anterior lung sliding, present A lines	Lung point where normal lung sliding resumes
Pneumonia		
Typical	Consolidation ± shred sign Adjacent pleural effusion	Dynamic air bronchograms Branching vascularity
Necrotizing		Non enhancing areas on CEUS
Atypical	Patchy or confluent B lines	Light beam artifact in COVID-19 pneumonia
Bronchiolitis	Subpleural consolidation Patchy or confluent B lines Thickened pleural line	
Cardiogenic pulmonary edema	Diffuse bilateral B lines ± bilateral pleural effusion	Cardiomegaly
RDS	Bilateral confluent B lines Patchy consolidation Thick irregular pleural line	
TTN	Diffuse bilateral B lines	Double lung point: compact B lines inferiorly, widely spaced B lines superiorly
MAS	Consolidations with air bronchograms	
Pulmonary sequestration	Solid echogenic mass, usually in lower lobes	Arterial supply from aorta or its branches
CPAM	Complex multicystic mass with interspersed solid component May be completely solid	

CPAM congenital pulmonary airway malformation, *MAS* meconium aspiration syndrome, *RDS* respiratory distress syndrome, *TTN* transient tachypnea of newborn

Supplementary Information The online version contains supplementary material available at https://doi.org/10.1007/s00247-022-05412-9.

Declarations

Conflicts of interest None

References

1. Lichtenstein D, Mézière G, Biderman P et al (1997) The comet-tail artifact. An ultrasound sign of alveolar-interstitial syndrome. Am J Respir Crit Care Med 156:1640–1646
2. De Martino L, Yousef N, Ben-Ammar R et al (2018) Lung ultrasound score predicts surfactant need in extremely preterm neonates. Pediatrics 142:e20180463
3. Brat R, Yousef N, Klifa R et al (2015) Lung ultrasonography score to evaluate oxygenation and surfactant need in neonates treated with continuous positive airway pressure. JAMA Pediatr 169:e151797
4. Pereda MA, Chavez MA, Hooper-Miele CC et al (2015) Lung ultrasound for the diagnosis of pneumonia in children: a meta-analysis. Pediatrics 135:714–722
5. Volpicelli G, Elbarbary M, Blaivas M et al (2012) International evidence-based recommendations for point-of-care lung ultrasound. Intensive Care Med 38:577–591
6. Kurepa D, Zaghloul N, Watkins L, Liu J (2018) Neonatal lung ultrasound exam guidelines. J Perinatol 38:11–22
7. Lichtenstein DA, Mauriat P (2012) Lung ultrasound in the critically ill neonate. Curr Pediatr Rev 8:217–223
8. Reali F, Sferrazza Papa GF, Carlucci P et al (2014) Can lung ultrasound replace chest radiography for the diagnosis of pneumonia in hospitalized children? Respir Inv Thorac Dis 88:112–115
9. Esposito S, Papa SS, Borzani I et al (2014) Performance of lung ultrasonography in children with community-acquired pneumonia. Ital J Pediatr 40:37
10. Lovrenski J (2012) Lung ultrasonography of pulmonary complications in preterm infants with respiratory distress syndrome. Ups J Med Sci 117:10–17
11. Pieper CH, Smith J, Brand EJ (2004) The value of ultrasound examination of the lungs in predicting bronchopulmonary dysplasia. Pediatr Radiol 34:227–231
12. Raimondi F, Migliaro F, Sodano A et al (2012) Can neonatal lung ultrasound monitor fluid clearance and predict the need of respiratory support? Crit Care 16:R220
13. Liu J, Chen X-X, Li X-W et al (2016) Lung ultrasonography to diagnose transient tachypnea of the newborn. Chest 149:1269–1275
14. Liu J, Cao H-Y, Fu W (2016) Lung ultrasonography to diagnose meconium aspiration syndrome of the newborn. J Int Med Res 44:1534–1542
15. Liu J, Wang Y, Fu W et al (2014) Diagnosis of neonatal transient tachypnea and its differentiation from respiratory distress syndrome using lung ultrasound. Medicine 93:e197
16. Brusa G, Savoia M, Vergine M et al (2015) Neonatal lung sonography: interobserver agreement between physician interpreters with varying levels of experience. J Ultrasound Med 34:1549–1554
17. Lichtenstein D (2009) Lung ultrasound in acute respiratory failure an introduction to the BLUE-protocol. Minerva Anestesiol 75:313–317
18. Lichtenstein DA, Mezière GA (2008) Relevance of lung ultrasound in the diagnosis of acute respiratory failure: the BLUE protocol. Chest 134:117–125

19. Biswas A, Lascano JE, Mehta HJ, Faruqi I (2017) The utility of the "shred sign" in the diagnosis of acute respiratory distress syndrome resulting from multifocal pneumonia. Am J Respir Crit Care Med 195:e20–e22
20. Lichtenstein DA (2009) Ultrasound examination of the lungs in the intensive care unit. Pediatr Crit Care Med 10:693–698
21. Reissig A, Copetti R, Mathis G et al (2012) Lung ultrasound in the diagnosis and follow-up of community-acquired pneumonia: a prospective, multicenter, diagnostic accuracy study. Chest 142:965–972
22. Trinavarat P, Riccabona M (2014) Potential of ultrasound in the pediatric chest. Eur J Radiol 83:1507–1518
23. Principi N, Esposito A, Giannitto C, Esposito S (2017) Lung ultrasonography to diagnose community-acquired pneumonia in children. BMC Pulm Med 17:212
24. Copetti R, Cattarossi L (2008) Ultrasound diagnosis of pneumonia in children. Radiol Med 113:190–198
25. Sperandeo M, Varriale A, Sperandeo G et al (2012) Assessment of ultrasound acoustic artifacts in patients with acute dyspnea: a multicenter study. Acta Radiol 53:885–892
26. Ambroggio L, Sucharew H, Rattan MS et al (2016) Lung ultrasonography: a viable alternative to chest radiography in children with suspected pneumonia? J Pediatr 176:93–98.e7
27. Chen H-J, Yu Y-H, Tu C-Y et al (2009) Ultrasound in peripheral pulmonary air-fluid lesions. Color Doppler imaging as an aid in differentiating empyema and abscess. Chest 135:1426–1432
28. James CA, Braswell LE, Pezeshkmehr AH et al (2017) Stratifying fibrinolytic dosing in pediatric parapneumonic effusion based on ultrasound grade correlation. Pediatr Radiol 47:89–95
29. Caiulo VA, Gargani L, Caiulo S et al (2011) Lung ultrasound in bronchiolitis: comparison with chest X-ray. Eur J Pediatr 170:1427–1433
30. Catalano D, Sperandeo M, Trovato G (2014) Re: Caiulo VA, Gargani L, Caiulo S, Fisicaro A, Moramarco F, Latini G, Picano E (2011) Lung ultrasound in bronchiolitis: comparison with chest X-ray. Eur J Pediatr. 2011;170:1427–33. Eur J Pediatr 173:405
31. Toma P (2013) Lung ultrasound in bronchiolitis. Eur J Pediatr 172:713
32. La Regina DP, Bloise S, Pepino D et al (2021) Lung ultrasound in bronchiolitis. Pediatr Pulmonol 56:234–239
33. Hafez MR, Sobh ES, Elsawy SB, Abo-Elkheir OI (2017) The usefulness of thoracic ultrasonography in diagnosis and staging of bronchogenic carcinoma. Ultrasound 25:200–212
34. Lichtenberger JP, Biko DM, Carter BW et al (2018) Primary lung tumors in children: radiologic–pathologic correlation from the radiologic pathology archives. Radiographics 38:2151–2172
35. Joshi P, Vasishta A, Gupta M (2019) Ultrasound of the pediatric chest. Br J Radiol 92:20190058
36. Jain R, Jana M, Gupta A, Naranje P (2021) Ultrasonography in the evaluation of pediatric chest "masses": when to consider? J Ultrasound Med 41:821–826
37. Williams HJ, Johnson KJ (2002) Imaging of congenital cystic lung lesions. Paediatr Respir Rev 3:120–127
38. Hernanz-Schulman M, Stein SM, Neblett WW et al (1991) Pulmonary sequestration: diagnosis with color Doppler sonography and a new theory of associated hydrothorax. Radiology 180:817–821
39. Stocker JT, Madewell JE, Drake RM (1977) Congenital cystic adenomatoid malformation of the lung. Classification and morphologic spectrum. Hum Pathol 8:155–171
40. Goh Y, Kapur J (2016) Sonography of the pediatric chest. J Ultrasound Med 35:1067–1080
41. Deganello A, Rafailidis V, Sellars ME et al (2017) Intravenous and intracavitary use of contrast-enhanced ultrasound in the evaluation and management of complicated pediatric pneumonia. J Ultrasound Med 36:1943–1954
42. Rafailidis V, Andronikou S, Mentzel H-J et al (2021) Contrast-enhanced ultrasound of pediatric lungs. Pediatr Radiol 51:2340–2350
43. Volpicelli G, Lamorte A, Villén T (2020) What's new in lung ultrasound during the COVID-19 pandemic. Intensive Care Med 46:1445–1448
44. Bouhemad B, Brisson H, Le-Guen M et al (2011) Bedside ultrasound assessment of positive end-expiratory pressure-induced lung recruitment. Am J Respir Crit Care Med 183:341–347
45. See KC, Ong V, Wong SH et al (2016) Lung ultrasound training: curriculum implementation and learning trajectory among respiratory therapists. Intensive Care Med 42:63–71
46. Lovrenski J (2020) Pediatric lung ultrasound — pros and potentials. Pediatr Radiol 50:306–313
47. Riccabona M, Laffan E (2018) Chest and lung ultrasound in childhood: applications, role, value and limitations. J Ultrason 18:281–283